Photochemistry of *p*-Benzoquinone Diazide Carboxylic Acids: Formation of 2,4-Didehydrophenols

**Wolfram Sander,*,† Götz Bucher,† Holger Wandel,† Elfi Kraka,*,‡
Dieter Cremer,‡ and William S. Sheldrick§**

*Contribution from the Lehrstuhl für Organische Chemie der Ruhr-Universität,
D-44780 Bochum, Germany, and Department of Theoretical Chemistry, University of Göteborg,
Kemigården 3, S-41296 Göteborg, Sweden*

Abstract: The photochemistry of *p*-benzoquinone diazide carboxylic acids (**7**) was studied using matrix isolation spectroscopy, product analysis, and high-level ab initio molecular orbital theory. The general photochemical pathway observed includes primary carbene formation, followed by secondary photodecarboxylation to yield derivatives of 2,4-didehydrophenol **9**. CCSD(T) calculations on the parent 2,4-didehydrophenol (**9a**) lead to an infrared spectrum which is in excellent agreement with the experimental one. Furthermore, calculations predict **9a** to be characterized by a distorted benzene ring with the hydroxy group pointing toward the radical center in *ortho* position. The heat of formation of **9a** is predicted to be 85 kcal/mol. Its formation from 1-oxo-2,5-cyclohexadien-4-ylidene-2-carboxylic acid (**8a**) by decarboxylation is exothermic by 30 kcal/mol where strong H-bonding in **8a** can be considered to facilitate the formation of **9a**.

Introduction

The chemistry of aromatic σ-biradicals (arynes) has been the subject of considerable interest throughout this century. Research on *o*-arynes started early with the pioneering work by Wittig,[1] and *o*-benzyne can now be considered a well-characterized molecule, which has been investigated extensively both with matrix isolation spectroscopy and with high-level ab initio calculations.[2] Recently, the focus of many research groups has shifted toward *p*-arynes and related diradicals, as these compounds are considered to be the critical intermediates in the DNA-cleaving reaction of enediyne antibiotics/cytostatica.[3,4] The natural enediyne cytostatica are optimized to fulfill under certain conditions a specific biologic task and not necessarily that of a useful anticancer drug. Therefore, ongoing research focuses on replacing the natural "warhead"[3] of the enediyne cytostatica, namely *p*-benzyne, by other highly reactive diradicals which are more suitable for an anticancer drug.[4]

The heats of formation of *o*-, *m*-, and *p*-benzyne have been determined by Wenthold and Squires[5] from collision-induced dissociation threshold energies to 106.6 ± 3.0, 122.0 ± 3.1, and 137.3 ± 3.3 kcal/mol, respectively, and are in excellent agreement with high level ab initio calculations.[6,26] Recently

Marquardt, Sander, and Kraka reported on the first matrix isolation and spectroscopic characterization of *m*-benzyne (**1**).[7] This aryne is more stable than *p*-benzyne and, accordingly, can be better handled in experiment. Because of this, **1** and its derivatives are of considerable interest for synthetic chemists, spectroscopists, structural chemists, and theoreticians.

In this contribution, we present results of our studies dealing with *m*-arynes. In particular, we concentrate on substituted *m*-arynes bearing hydroxy groups, i.e., 2,4-didehydrophenols. These reactive intermediates were generated by sequential photodediazotation and photodecarboxylation of appropriate *p*-benzoquinone diazide carboxylic acids and investigated by matrix isolation spectroscopy in connection with product studies.

m-Benzyne can be depicted as either an aromatic σ-biradical **1** or as bicyclo[3.1.0]hexatriene (**2**). The literature provides evidence for both structures: Washburn et al. investigated the dehydrobromination of dibromobicyclo[3.1.0]hexene (**3**) and

† Lehrstuhl für Organische Chemie, Ruhr-Universität Bochum.
‡ University of Göteborg.
§ Lehrstuhl für Analytische Chemie, Ruhr-Universität Bochum.
⊗ Abstract published in *Advance ACS Abstracts,* October 1, 1997.
(1) Wittig, G. *Naturwissenschaften* **1942,** 696−703.
(2) Radziszewski, J. G.; Hess, B. A. J.; Zahradnik, R. *J. Am. Chem. Soc.* **1992,** *114,* 52−57.
(3) Nicolaou, K. C.; Dai, W. M. *Angew. Chem.* **1991,** *103,* 1453−81; *Angew. Chem., Int. Ed. Engl.* **1991,** *30,* 1387−1415.
(4) Chen, P. *Angew. Chem.* **1996,** *108,* 1584−1586; *Angew. Chem., Int. Ed. Engl.* **1996,** *35,* 1478−1480.
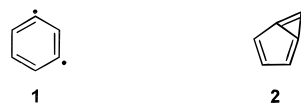(5) Wenthold, P. G.; Squires, R. R. *J. Am. Chem. Soc.* **1994,** *116,* 6401−6412.
(6) Cramer, C. J.; Nash, J. J.; Squires, R. R., *Chem. Phys. Lett.*, in press.
(7) Marquardt, R.; Sander, W.; Kraka, E. *Angew. Chem.* **1996,** *35,* 746−748; *Angew. Chem., Int. Ed. Engl.* **1996,** *35,* 746−748.
(8) (a) Washburn, W. N.; Zahler, R. *J. Am. Chem. Soc.* **1976,** *98,* 7827−7828. (b) Washburn, W. N.; Zahler, R. *J. Am. Chem. Soc.* **1976,** *98,* 7828−7830. (c) Washburn, W. N. *J. Am. Chem. Soc.* **1975,** *97,* 1615−1616.
(9) Billups, W. E.; Buynak, J. D.; Butler, D. *J. Org. Chem.* **1979,** *44,* 4218−4219.

(10) Bucher, G.; Sander, W.; Kraka, E.; Cremer, D. *Angew. Chem.* **1992,** *104,* 1225−1228; *Angew. Chem., Int. Ed. Engl.* **1992,** *31,* 1230−1233.
(11) Bucher, G.; Sander, W. *Chem. Ber.* **1992,** *125,* 1851−1859.
(12) Sander, W. *Angew. Chem.* **1990,** *102,* 362−72; *Angew. Chem., Int. Ed. Engl.* **1990,** *29,* 344−354.
(13) Bucher, G. Studien auf der C6H4O-Hyperfläche. Dissertation, TU Braunschweig, 1992.
(14) Sander, W.; Bucher, G.; Reichel, F.; Cremer, D. *J. Am. Chem. Soc.* **1991,** *113,* 5311−5322.
(15) Bucher, G.; Sander, W. *J. Org. Chem.* **1992,** *57,* 1346−1351.
(16) Sander, W.; Bucher, G.; Komnick, P.; Morawietz, J.; Bubenitschek, P.; Jones, P. G.; Chrapkowski, A. *Chem. Ber.* **1993,** *126,* 2101−2109.
(17) Komnick, P.; Sander, W. *Liebigs Ann.* **1996,** *114,* 7−9.
(18) Sues, O. *Liebigs Ann. Chem.* **1944,** *556,* 65−84.
(19) Tsuda, M.; Oikawa, S. *J. Photopolym. Sci. Technol.* **1989,** *2,* 325−339.
(20) Reiser, A.; Shih, H.-Y.; Yeh, T.-F.; Huang, J.-P. *Angew. Chem.* **1996,** *108,* 2611−2622; *Angew. Chem., Int. Ed. Engl.* **1996,** *35,* 2428−2440.
(21) Becke, A. J. *Chem. Phys.* **1993,** *98,* 5648−5652.
(22) Stephens, P. J.; Devlin, F. J.; Chabalowski, C. F.; Frisch, M. J. *J. Phys. Chem.* **1993,** *98,* 11623.
(23) Hariharan, P. C.; Pople, J. A. *Chem. Phys. Lett.* **1972,** *66,* 217−219.
(24) Raghavachari, K.; Trucks, G. W.; Pople, J. A.; Head-Gordon, M. *Chem. Phys. Lett.* **1989,** *157,* 479−483.
(25) Cox, J. D.; Pilcher, G. *Thermochemistry of Organic; Organometallic Compounds*; Academic Press: New York, 1970.
(26) Kraka, E.; Cremer, D. *Chem. Phys. Lett.* **1993,** *216,* 333−340.

Scheme 1

obtained trapping evidence for **2**,[8] while Billups et al., on the other hand, obtained trapping products from the *m*-dehydronaphthalene **4**, although a synthesis of the corresponding bicyclo[3.1.0]hexatriene system had been attempted.[9]
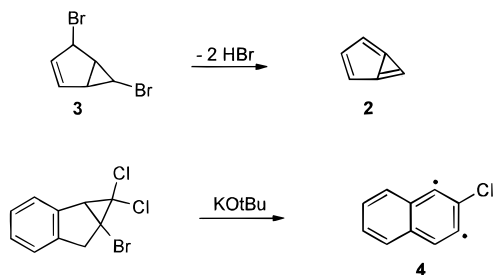
Thus, the question whether structure **1** or **2** represents the true formula of *m*-benzyne remained unanswered until recently, when the spectroscopic characterization of *m*-benzyne by Marquardt, Sander, and Kraka revealed that this molecule is in fact best described as the aromatic σ-biradical **1**. Aryne **1** was generated in argon matrix at 10 K from two independent precursors: both flash vacuum pyrolysis of isophthaloyl diacetyldiperoxide **5** and photolysis of matrix-isolated cyclophane **6** yielded, among other products, benzyne **1**. The structural assignment could be confirmed by correlation of the experimental infrared spectrum with a spectrum obtained by CCSD-(T) ab initio calculations.
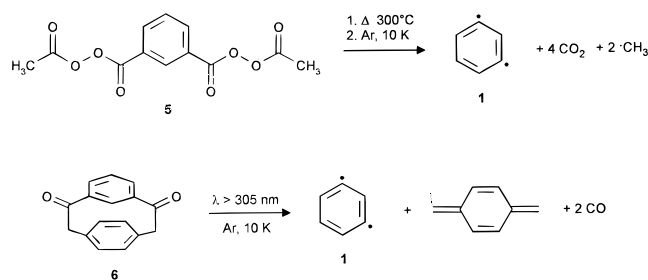

According to the calculations, *m*-benzyne (**1**) is best described as a planar distorted hexagon, in which the intra-annular C1–C3 distance is somewhat shortened, giving evidence for considerable interaction between the radical centers. In a recent communication, we also described the matrix isolation of 2,4-didehydrophenol (**9a**), starting from *p*-benzoquinone diazide carboxylic acid (**7a**) via carbene **8a**. Its geometry, as calculated on the GVB 6-31G(d) level, is very similar to that of the parent *m*-benzyne and the bicyclic isomer **10a** was excluded.[10] In the
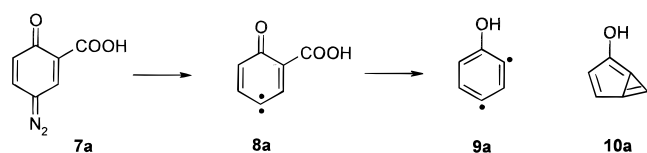
minimum energy conformation, the hydroxy group points toward the *ortho* radical center, indicating a stabilizing interaction. Thus, the substituted *m*-benzyne **9** represents an interesting model system for the study of the interaction of aromatic singlet biradicals with substituents. The corresponding quinone diazides with a variety of substituents are readily accessible precursors of substituted dehydrophenols **9**. In addition, since the benzynes **9** are formed on visible light irradiation of quinone
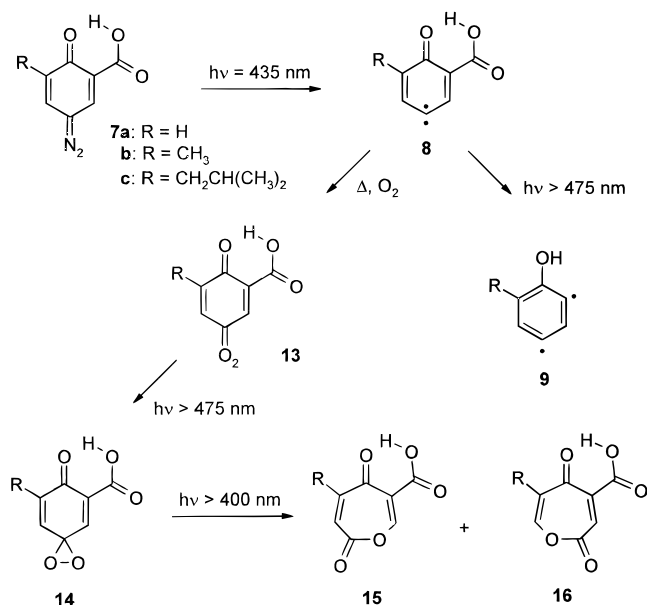
diazides **7**, this procedure might provide a viable route to study the solution chemistry of *m*-benzynes.

The goal of this study is to gain further insights into the mechanism of the photodecarboxylation of carbene **8a**, to investigate the electronic structure of **9a** by high-level ab initio theory, to characterize some of its substituted derivatives **9** spectroscopically, and to investigate its solution reactivity.

Results

**4-Diazo-1-oxocyclohexa-2,5-diene-2-carboxylic Acid (7a).** The photochemistry of **7a** has already been briefly described in a preliminary communication.[10] Matrix isolation of **7a** could be achieved by subliming the diazo compound in an electrically heated oven at 136 °C and 10^{-5} mbar. Even under optimized conditions, however, the sublimation of the highly polar **7a** (and, in analogy, all other quinone diazide carboxylic acids investigated in the present study) remained difficult, and only modest amounts could be brought into the gas phase.

In initial experiments, **7a** was irradiated using broad-band visible light ($\lambda > 475$ nm). Under these conditions, **7a** decomposes rapidly and a new product (A) with a characteristic IR absorption at 3612 cm^{-1}, indicating a hydroxy functionality, appears together with an intense CO_2 band. This new compound, however, does not show a prominent band in the carbonyl region. Under more selective conditions (monochromatic irradiation, $\lambda = 435$ nm), another product (B) is formed, which still exhibits a band characteristic of a carboxylic acid ($\nu = 1758$ cm^{-1}). This compound decarboxylates photochemically with orange or red light (complete conversion in less than 1 min with $\lambda > 475$ nm, slow conversion with $\lambda > 780$ nm) and yields the same hydroxy compound (A) found in the initial experiments (Figure 1, Scheme 1)). In separate experiments using oxygen-doped argon matrices (typically 1% O$_2$ in Ar), product B could be identified as triplet carbene **8a** by oxygen trapping.[11] The formation of carbonyl *O*-oxides by the thermal reaction of carbenes with $^3O_2$ is highly characteristic and frequently used to identify matrix-isolated carbenes.[12]

When a sample of **8a**, matrix isolated in argon doped with 1% O$_2$, is briefly warmed to 40 K, the matrix becomes intensely yellow. The assignment of the primary oxidation product as carbonyl *O*-oxide **13a** can be justified by the intense color (λ_{max} = 440 nm, Ar, 10 K) and the strong IR absorption at 1082 cm^{-1}, characteristic of the O–O stretching vibration of a
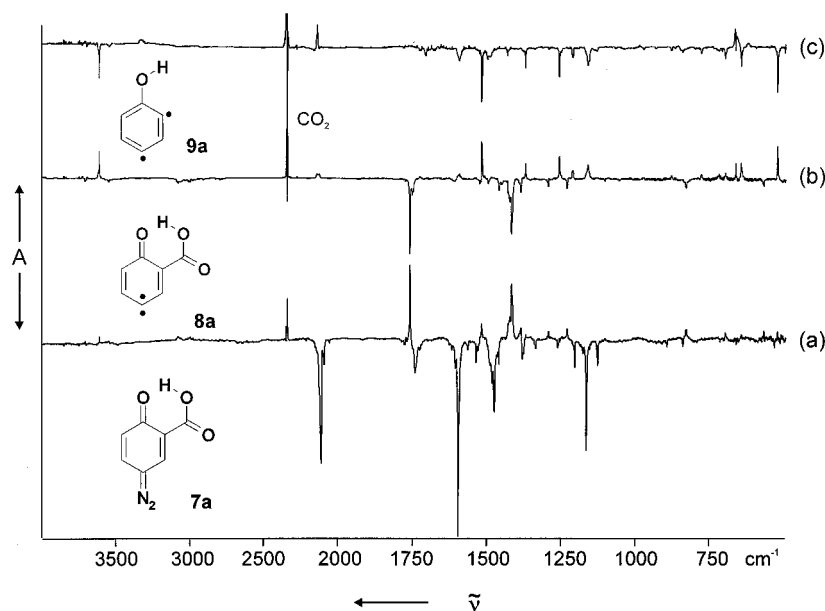
Figure 1. IR difference spectra showing the photochemistry of **7a** in argon at 10 K. (a) Bottom: bands of quinone diazide **7a** disappearing on irradiation ($\lambda = 435$ nm, 20 min). Top: bands of carbene **8a** and small amounts of **9a** and CO_2 appearing. (b) Bottom: bands of **8a** disappearing on irradiation ($\lambda > 475$ nm, 30 min). Top: bands of didehydrophenol **9a** and CO_2 appearing. (c) Bottom: bands of **9a** disappearing on irradiation ($\lambda > 260$ nm, 1 h). Top: bands appearing, assigned to a ketene of unknown structure.
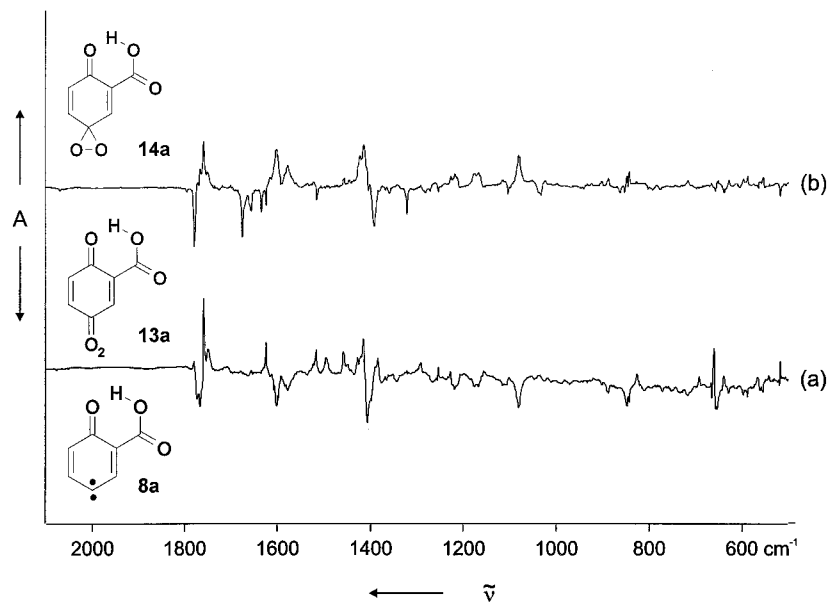
Figure 2. IR difference spectra showing the oxygenation of carbene **8a** in a 2% O_2-doped argon matrix and subsequent photochemistry. (a) Bottom: bands of **8a** disappearing on annealing at 35−45 K. Top: bands of carbonyl oxide **13a** appearing. (b) Bottom: bands of **13a** disappearing on irradiation ($\lambda > 515$ nm, 1 min). Top: bands of dioxirane **14a** appearing.

quinone *O*-oxide.[11] When $^{18}O_2$ was used in these experiments the absorption was red-shifted to 1034 cm^{-1}. Irradiation of quinone *O*-oxide **13a** with orange light ($\lambda > 515$ nm) results in the rapid conversion to dioxirane **14a** (Figure 2). The dioxirane **14a**, in turn, is also photolabile and converted to a mixture of lactones **15a** and **16a**[13] by irradiation with blue light ($\lambda > 400$ nm).

Product A is formed from carbene **8a** by photodecarboxylation. Simultaneously the hydrogen shift from the carboxy group to the keto functionality of carbene **8a** occurs. Additional evidence for this rearrangement comes from the investigation of the partially deuterated quinone diazide **8a**-d_1. In this case, the hydroxy stretching frequency in product A is shifted to 2666 cm^{-1}.

The infrared spectrum of product A offers no indication of the presence of a ketene, alkyne, or allene functionality, which would be the product of a ring opening reaction. Given this,

two structures remain to be discussed: 2,4-didehydrophenol (**9a**) and bicyclo[3.1.0]hexatriene-2-ol (**10a**).

A discrimination between these two possibilities was only possible by ab initio molecular orbital theory, see below. These studies gave unequivocal evidence that 2,4-didehydrophenol (**9a**) was indeed the intermediate observed by us (Figure 3).

Upon UV irradiation ($\lambda > 260$ nm), biradical **9a** proved to be photolabile. However, it was not possible to characterize the product formed, as a large peak at 2138 cm^{-1}, very close to the absorption of matrix-isolated carbon monoxide, is the only strong feature in the IR spectrum. (Further weak bands: 1419, 1047, and 963 cm^{-1}.) Thus, the photoproduct of **9a** is likely to be a ketene, but its structure remains unclear.

The photochemistry of **7a** in an argon matrix was also studied by UV−vis detection. Carbene **8a** shows a weak and very broad absorption starting from ca. 400 nm tailing out into the red, a medium-intensity, relatively sharp maximum at 390 nm (this is
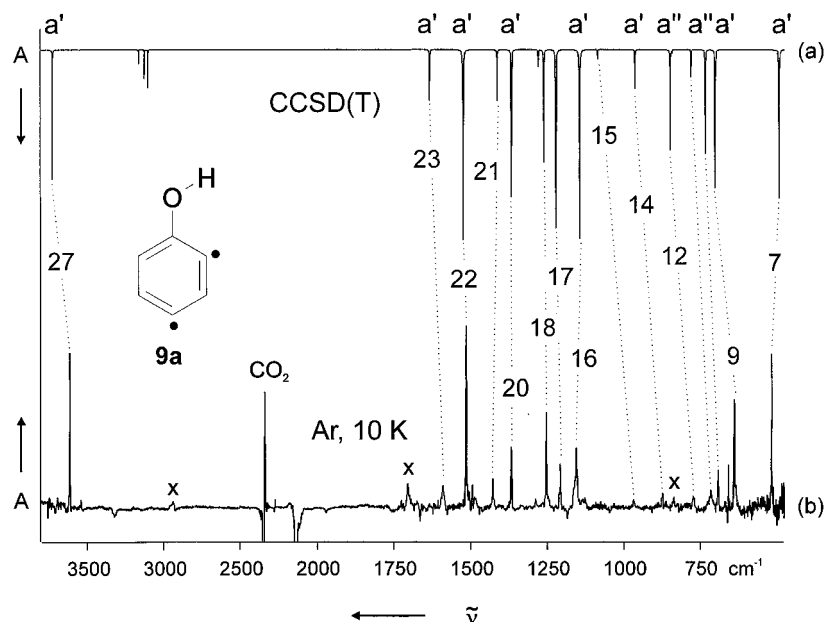
Figure 3. IR spectrum of 2,4-didehydrophenol **9a**. (a) Spectrum of **9a** calculated with CCSD(T). The band positions are scaled with 0.96. (b) Difference spectrum showing the $\lambda > 260$ nm photochemistry of **9a**. Bands pointing up are assigned to **9a**. x: unknown impurities.
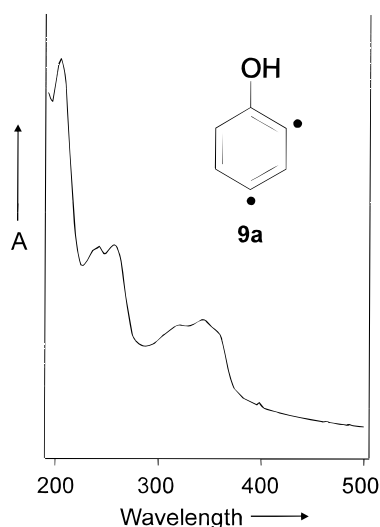

**Figure 4.** UV−vis spectrum of didehydropenol **9a** in argon at 10 K.

a feature characteristic of 4-oxocyclohexadienylidenes),[14,15] and strong bands at 356, 344, 316, and 308 nm. The UV−vis spectrum of biradical **9a** is similar: bands are found with λ_{max} = 356 (sh), 344, 318, 304 (sh), 256, and 238 nm (Figure 4), but there is no band discernible at $\lambda > 400$ nm, although the compound undergoes a photochemical transformation when irradiated with these wavelengths.

Product studies with quinone diazide **7a** were difficult because of the extremely low solubility of **7a** in common solvents. One of the few solvents which allowed for convenient concentrations of **7a** is 1,1,1-trifluoroethanol. In this case, the main product is 5-(2,2,2-trifluoroethoxy)salicylic acid, derived from the insertion of the intermediate singlet carbene into the O−H bond. Interestingly, significant amounts (ca. 10%) of 5-fluorosalicylic acid are also formed. Insertion into carbon−fluorine bonds is a very uncommon reaction, even for highly reactive singlet carbenes. In a control experiment, 4-oxocyclohexadienylidene (**12a**) was generated by irradiation of quinone diazide **11a** in 1,1,1-trifluoroethanol. While the yield of 4-fluorophenol is less than 1% in this case, the photolysis of 4-hydroxybenzene-diazonium chloride under otherwise identical conditions results in a 1:1 mixture of 4-fluorophenol and 4-trifluoroethoxyphenol. Obviously, reactivity toward C−F bonds is a property charac-

teristic of diazonium salts, which indicates that **7a** must be at least partially protonated in 1,1,1-trifluoroethanol.
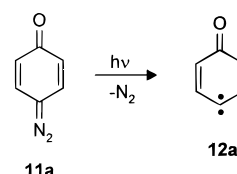
6-Alkyl-Substituted Derivatives 7. To characterize some derivatives of *m*-benzyne **9a** and to improve the solubility of the corresponding diazo compounds in common solvents such as MTHF, we synthesized a series of *p*-benzoquinone diazide carboxylic acids (**7**) with alkyl substituents in 6-position. While the solubility of the 6-methyl-substituted diazo compound **7b** in MTHF was still unsatisfactory, detailed product studies were possible with the 6-isobutyl-substituted diazo compound **7c**.
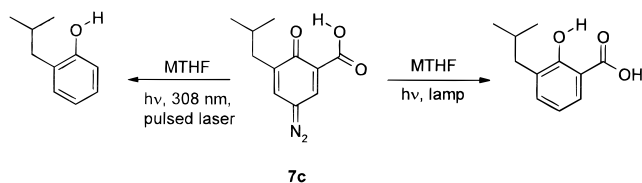
Thus, when **7c** is irradiated in MTHF solution at room temperature or glass at 77 K using a mercury high-pressure arc lamp, the main product is 3-isobutylsalicylic acid (which is the product formed via hydrogen abstraction by the carbene), while 308 nm pulsed laser irradiation of **7c** yields a significant amount (up to 30%, depending on the reaction conditions) of 2-iso-butylphenol, a product derived from *m*-aryne **9c**. Irradiation in ethanol at room temperature or 77 K exclusively yields trapping products of carbene **8c** (OH insertion and H abstraction) and no decarboxylation.

As with the parent diazo compound **7a**, the alkyl-substituted derivatives **7b,c** were also studied by matrix isolation spectros-copy. Because the melting points of **7b,c** are lower than that of parent diazo compound **7a**, we had initially hoped for a higher volatility of **7b,c** as compared to **7a**. However, concurrently with the melting point, also the temperature of decomposition was lowered upon alkyl substitution, so that the amounts of
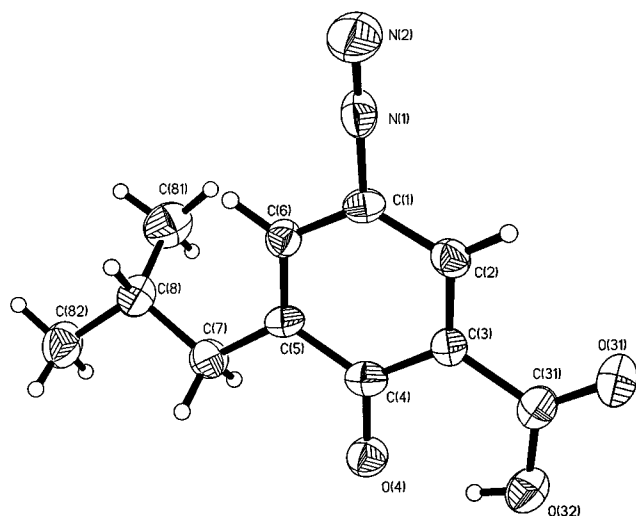
Figure 5. Structure of **7c** as determined by X-ray crystallography.

Table 1. Selected Interatomic Distances (Å) in **7a**[16] and **7c** (Standard Deviation).

	7a	7c
C(1)−C(2)	1.396(4)	1.390(7)
C(2)−C(3)	1.362(4)	1.397(7)
C(3)−C(4)	1.450(3)	1.431(7)
C(4)−C(5)	1.426(4)	1.455(7)
C(5)−C(6)	1.356(4)	1.357(6)
C(6)−C(1)	1.416(4)	1.405(7)
C(4)−O(4)	1.285(3)	1.293(6)
C(3)−C(31)	1.496(4)	1.495(7)
C(31)−O(31)	1.208(4)	1.229(6)
C(31)−O(32)	1.332(4)	1.321(6)
C(1)−N(1)	1.368(4)	1.391(7)
N(1)−N(2)	1.102(4)	1.109(6)
O(4)−O(32)	2.475	2.442

Table 2. Selected Bond Angles (deg) in **7a**[16] and **7c** (Standard Deviation)

	7a	7c
C(1)−C(2)−C(3)	118.9(3)	116.4(5)
C(2)−C(3)−C(4)	120.7(2)	121.2(2)
C(3)−C(4)−C(5)	117.7(2)	119.8(5)
C(4)−C(5)−C(6)	121.7(2)	117.7(5)
C(5)−C(6)−C(1)	118.3(2)	121.0(5)
C(6)−C(1)−C(2)	122.6(2)	123.9(5)
O(4)−C(4)−C(3)	120.9(2)	119.7(5)
C(4)−C(3)−C(31)	120.5(2)	119.9(5)
C(3)−C(31)−O(31)	123.3(2)	121.7(5)
O(31)−C(31)−O(32)	121.8(2)	122.0(5)
C(6)−C1)−N(1)	119.4(2)	118.6(5)
C(1)−N(1)−N(2)	178.8(3)	177.8(6)

diazo compounds **7b,c** that could be sublimed were even smaller than that of **7a**.

The photochemical behavior of diazo compounds **7b,c** in Ar matrix is analogous to that of **7a**. Monochromatic photolysis ($\lambda = 435$ nm) of the diazo compounds yields the corresponding carbene carboxylic acids **8b,c** (Scheme 1), which could be photochemically decarboxylated with orange or red light. The resulting *m*-arynes **9b,c** show prominent ν_{O-H} bands at 3612 (**9b**) or 3613 cm^{-1} (**9c**). In the case of **9b**-d_1, ν_{O-D} is found at $\nu = 2666$ cm^{-1}—at exactly the same position as in the parent compound **9a**-d_1. The reactivity of carbenes **8b,c** toward molecular oxygen is analogous to the reactivity of **8a**; the corresponding quinone *O*-oxides **13b,c** are obtained by annealing argon matrices containing the carbenes and 1−2% oxygen at ca. 40 K. Irradiation ($\lambda > 515$ nm) of the intensely yellow **13b** (λ_{max}(Ar, 10 K) = 464 nm) produces dioxirane **14b**, which in turn is photochemically converted into a mixture of the lactones **15b** and **16b**.[13] Infrared data for these compounds are listed in the Experimental Section.

Diazo compound **7c** was characterized by X-ray crystallography. The structure clearly reveals the presence of an intramolecular hydrogen bridge, as in the case of parent compound **7a**.[16] The distance between the keto oxygen atom (O4 in Figure 5) and the hydroxy oxygen atom in the carboxy functionality (O32) is only 2.442 Å and thus even shorter than the corresponding OO distance in **7a** (2.475 Å). The ketocarbonyl bond length C4−O4 is unusually long (1.293 Å), indicating a bond order of significantly less than 2. The N≡N bond length is in a range typical for *p*-benzoquinone diazides (**7c**, 1.109 Å; **7a**, 1.102 Å; *p*-benzoquinone diazide **11a**, 1.115 Å).[16] Diazo compound **7c** has an essentially planar structure, but unlike in the case of **7a**, which can crystallize in a very dense layered structure (and is thus very hard to dissolve in common solvents, like MTHF),[16] the isobutyl substituents somewhat reduce the density of crystal packing, so that **7c** is sufficiently soluble in MTHF. Tables 1 and 2 give an overview of selected geometric parameters in **7c**.

1,4-Naphthoquinone Diazide 2-Carboxylic Acid (7d). When **7d**, matrix-isolated in Ar at 10 K, is irradiated with monochromatic light ($\lambda = 435 \pm 5$ nm), carbene **8d** ($\nu_{C=O,carboxy}$ = 1753 cm^{-1}, $\nu_{C=O,keto}$ = 1429 cm^{-1}) was obtained in quantitative yield, which in turn could be converted into *m*-aryne **9d** by yellow light irradiation ($\lambda > 475$ nm) (Figure 6, Scheme 2). Biradical **9d** shows a characteristic ν_{O-H} at 3608 cm^{-1} (ν_{O-D} = 2663 cm^{-1}), thus slightly shifted relative to dehydrophenol **9a**. Interesting, as with carbene **8a**, is the low frequency of the C=O stretch vibration of the cyclohexadienone chromophor (the

frequency observed indicates a bond order of ca. 1.5), which indicates that the contribution of the 4-naphthyl-1-naphthoxy biradical mesomeric structure must be significant. In the UV− vis regime, the characteristic feature of carbene **8d** is a weak and broad absorption between ca. 425 and 600 nm, in addition to two strong maxima at 342 and 358 nm, similar to the UV− vis spectrum of the corresponding carbene without carboxy function in 2-position.[15] If **8d** is converted to **9d**, the broad band in the visible portion of the spectrum disappears, while the remainder of the spectrum remains virtually unchanged.

Upon warming an oxygen-doped Ar matrix to 40 K, carbene **8d** reacts readily with $^3O_2$ to yield the corresponding deep red carbonyl *O*-oxide **13d** (characteristic broad absorption between 400 and 600 nm), which confirms our assignment for **8d**.

Biradical **9d** proved to be photolabile. After photolysis (λ = 248 nm), several infrared bands appeared that can be assigned to a mixture of indeneketene and indenylidene (Scheme 3). The same set of bands were observed upon photolysis of 1,4-naphthoquinone diazide **11b** in an Ar matrix,[17] and therefore, it is tempting to postulate the rearrangement of **9d** to carbene **12b** as the primary step of the short-wavelength UV photolysis. Carbene **12b** is not stable under these conditions[17] and thus not observed.

Photolysis (350−450 nm) of **7d** in ethanol or EPA at room temperature resulted in the formation of 1-hydroxy-2-naphthoic acid and 4-ethoxy-1-hydroxy-2-naphthoic acid (GC analysis of the methyl esters obtained by treatment of the photoproducts with diazomethane). Thus, as with the alkyl-substituted derivatives **7b,c**, decarboxylation is slow compared to the trapping of the carbene and only products derived from carbene **8d**—and not from diradical **9d**—are formed.

1,2-Naphthoquinone 1-Diazide 3-Carboxylic Acid (18). When *o*-quinone diazides are photolyzed, they usually undergo a rapid Wolff rearrangement to yield indene ketenes. This reaction is called the Süs reaction[18] and is basis of the chemistry of *o*-naphthoquinone diazide photoresists.[19,20] We reasoned that
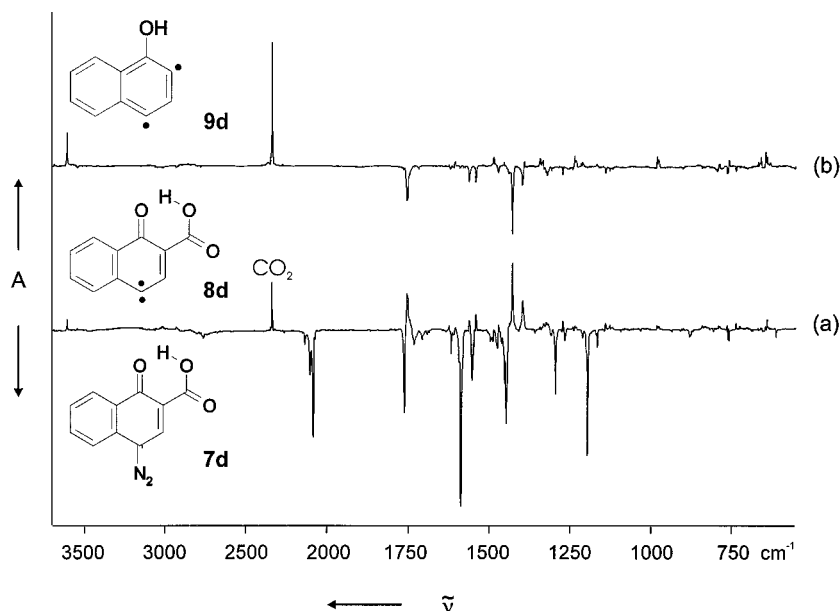
Figure 6. IR difference spectra showing the photochemistry of diazo compound **7d** in argon at 10 K. (a) Bottom: bands of quinone diazide **7d** disappearing on irradiation (λ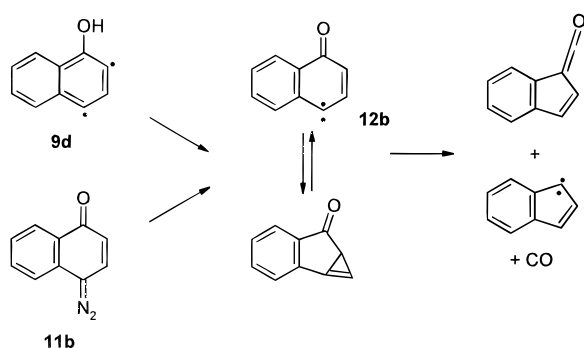 = 435 nm, 20 min). Top: bands of carbene **8d** and small amounts of **9d** and CO_2 appearing. (b) Bottom: bands of **8d** disappearing on irradiation (λ > 475 nm, 30 min). Top: bands of didehydrophenol **9d** and CO_2 appearing.

Scheme 2
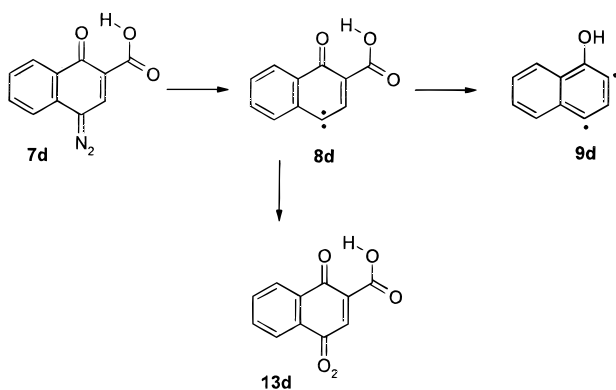

Scheme 3

the Wolff rearrangement might be retarded if the carbonyl group of the intermediary singlet ketocarbene was involved in an intramolecular hydrogen bond. In the hope to obtain evidence for photodecarboxylation also in 2-oxocyclohexadienylidene-3-carboxylic acids, we synthesized the *o*-naphthoquinone diazide **18** and investigated its photochemistry in an Ar matrix at 10
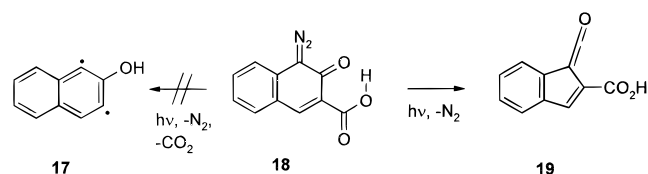

K. Fortunately, **18** was much easier to sublime than, for instance, the corresponding *p*-derivative **7d**, which is likely due to its reduced dipole moment. However, we did not obtain evidence for photodecarboxylation yielding biradical **17**. The exclusive product observed was tentatively assigned to indene ketene **19** (typical IR bands: 3570, 2142, 1758 cm^{-1}, Figure 7), and carbon dioxide was not formed.

While the absence of a detectable ν_{O-H} makes is likely that an intramolecular hydrogen bond is indeed present in quinone diazide carboxylic acid **18** (and thus also in the resulting singlet ketocarbene), it is evident that this hydrogen bond is not strong enough to sufficiently slow the Wolff rearrangement. Even under high-energy pulsed laser (KrF Excimer Laser, 248 nm, 250 mJ/pulse) conditions, no photodecarboxylation was observed.

Quantum Chemical Calculations

For **1**, **2**, **9a**, and **10a**, density functional theory (DFT) and coupled cluster (CC) theory was used to get reasonable geometries and to clarify the question whether the biradical or bicyclic forms are more stable in these cases. At the UB3LYP/6-31G(d,p)[21−23] level of theory (unrestricted DFT with a hybrid functional) a stationary point was found for each of the four molecules. However, at the more reliable CCSD(T)/6-31G(d,p) level of theory (CC calculations with all single and double excitations and a perturbative treatment of the triple excitations[24]), no minimum was found for the bicyclic forms **2** and **10a** and only the σ-biradicals **1** and **9a** turned out to be stable. The CCSD(T) geometrical parameters are shown in Figure 8, while the corresponding UB3LYP/6-31G(d,p) values are listed in Table 3. (The numbering of the ring atoms in **1** and phenol is adjusted to that in **9a**.)

Hydroxyl substitution leads to little changes in the geometry of **1**. The ring keeps the same distorted form of a hexagon, and the bond lengths of **1** and **9a** are almost identical (Figure 8). The OH group takes a position in the ring plane with the H atom directed toward the radical center because steric repulsion is minimized in this way. Rotation of the OH group is hindered by a barrier of 4.6 kcal/mol (UB3LYP/6-31G(d,p) geometry optimizations) which corresponds to a CCOH rotational angle of 90°. The confirmation with the H(O) atom directed toward C6H is 3.4 kcal/mol higher in energy than the equilibrium form
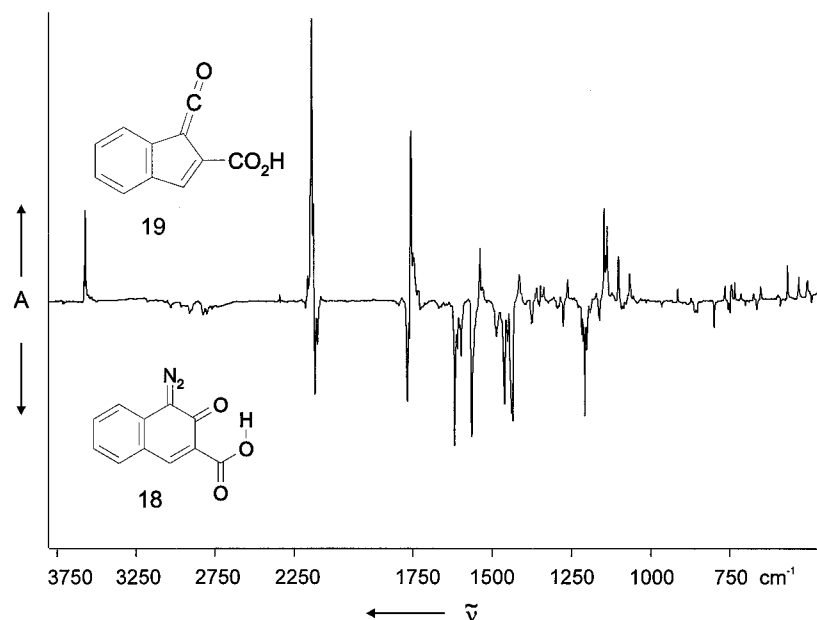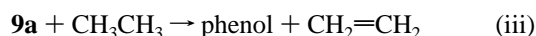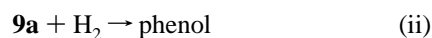
Figure 7. IR difference spectrum showing the photochemistry of **18** in argon at 10 K. Bottom: bands of **18** disappearing on irradiation ($\lambda > 420$ nm, 50 min). Top: bands appearing, tentatively assigned to indeneketene **19**.
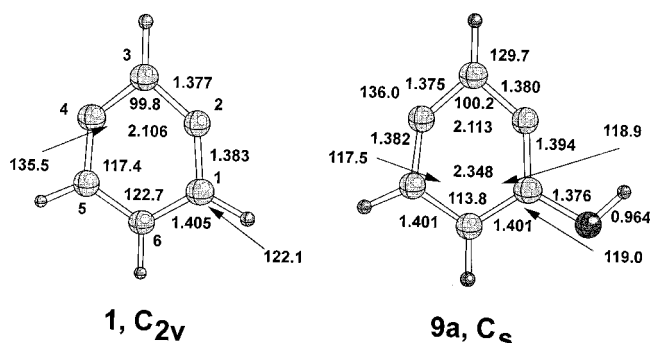
Figure 8. CCSD(T)/6-31G(d,p) geometry of *m*-benzyne (**1**) and 2,4-dehydrophenol (**9a**). Distances in angstroms and angles in degrees.

of **9a**. At the same level of theory, the rotational barrier of the OH group in phenol is calculated to be 4.1 kcal/mol.

The stability of **9a** can be determined with the help of the formal reactions i−iii:

$$1 + \text{phenol} \rightarrow \textbf{9a} + \text{benzene} \qquad (i)$$

$$\textbf{9a} + H_2 \rightarrow \text{phenol} \qquad (ii)$$

$$\textbf{9a} + CH_3CH_3 \rightarrow \text{phenol} + CH_2{=}CH_2 \qquad (iii)$$

For this purpose, B3LYP/6-31G(d,p) reaction energies have been corrected by differences in the appropriate zero point energies (ZPE) and checked by comparing with CCSD(T) reaction energies. By combining the reaction enthalpies obtained in this way with known reaction enthalpies of benzene (19.8),[25] phenol (−23.0),[25] *m*-benzyne (122.8),[26] ethane (−20.2),[25] and ethene (12.4 kcal/mol),[25] one gets from reaction i a $\Delta H_f°$ value of 83.4 kcal/mol for **9a**, from reaction ii 86.0, and from reaction iii 85.5 kcal/mol, respectively. In view of the relatively large uncertainty of $\Delta H_f°$ for **1**, we suggest a value of 85 ± 1 kcal/mol.

Substituting **1** by an OH group as in **9a** is 3.4 kcal/mol less stabilizing than substituting benzene by an OH group (total stabilization energy: 14.4 kcal/mol at B3LYP/6-31G(d,p). While both *m*-benzynes **1** and **9a** are stabilized by through-space and through-bond interaction as well as reduced steric interactions between the CH groups, π-delocalization and through-bond interactions are opposing each other, which

Table 3. Adiabatic Frequencies for Phenol, 2,4-Dehydrophenol (**9a**), and *m*-Benzyne (**1**)[a]

	phenol		9a		1	
	r, α, τ	ω	r, α, τ	ω	r, α, τ	ω
	A. Stretching Modes					
C1C2	1.399	1350	1.385	1349	1.375	1381
C2C3	1.395	1367	1.376	1303	1.375	1218
C3C4	1.395	1371	1.377	1255	1.375	1218
C4C5	1.397	1361	1.374	1379	1.375	1381
C5C6	1.393	1379	1.400	1350	1.403	1335
C6C1	1.399	1353	1.405	1333	1.403	1335
C1O7	1.368	1219	1.370	1212	1.086	3193
O7H	0.966	3815	0.967	3809		
	B. Bending Modes					
C6C1C2	120.0	945	118.2	874	117.3	826
C1C2C3	119.8	920	131.5	583	134.0	404
C2C3C4	120.5	921	103.9	448	101.9	314
C3C4C5	119.3	932	133.0	498	134.0	404
C4C5C6	120.8	922	117.5	832	117.3	826
C5C6C1	119.6	925	115.7	789	115.5	704
C2C1O7	122.6	707	122.7	670	121.1	1279
C1O7H	109.0	1274	108.1	1269		
C2C3H	119.3	1333	127.9	1271	129.0	1270
C6C5H	119.2	1335	121.5	1280	121.6	1279
C1C6H	118.9	1299	121.0	1282	122.3	1308
	C. Torsional Modes					
C6C1C2C3	0	554	0	526	0	573
C1C2C3C4	0	581	0	491	0	531
C2C3C4C5	0	593	0	489	0	531
C3C4C5C6	0	592	0	540	0	573
C4C5C6C1	0	584	0	544	0	561
C5C6C1C2	0	557	0	524	0	561
C2C1O7H	0	373	0	383		

[a] Distances in Å, angles in deg, frequencies in cm^{-1}. For the numbering of atoms, see Figure 8.

explains the somewhat lower stabilization effect of the OH group in the case of dehydrophenol **9a**.
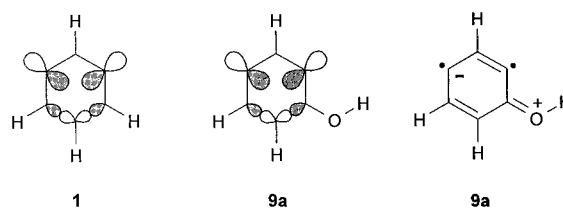
Table 4. Calculated and Measured Vibrational Frequencies ω and Infrared Intensities I of *m*-Benzyne (**1**) and 2,4-Dehydrophenol (**9A**)

| | | m-Benzyne (**1**) | | | | | | | | 2,4-Dehydrophenol (**9a**) | | | | | |
| | | CCSD(T) | | B3LYP | | exptl | | | | CCSD(T) | | B3LYP | | exptl | |
no.	sym	ω	I	ω	I	ω	I	no.	aym	ω	I	ω	I	ω	I
1	b$_1$	367	4.6	387	4.1			1	a″	251	0.0	259	0.0		
2	a$_1$	386	5.7	233	1.3			2	a″	320	133.3	358	126.7		
3	b$_1$	479	0	583	10.6			3	a′	332	7.7	300	20.8		
4	a$_2$	497	0	505	0			4	a″	356	5.3	389	4.0		
5	b$_2$	545	104.1	567	74.7	547	100	5	a′	436	1.3	420	2.0		
6	b$_1$	743	56.4	768	46.3	751	45	6	a″	445	2.4	504	4.2		
7	b$_1$	818	10.7	837	5.5	824	20	7	a′	516	65.4	541	32.4	518.8	s
8	a$_2$	824	0	845	0			8	a″	530	0.3	632	2.4		
9	a$_1$	849	0.8	856	0.2			9	a′	735	58.0	745	63.2	641.2	s
10	b$_1$	918	0.0	972	0.8			10	a″	769	37.4	796	36.1	694.7	m
11	b$_2$	975	29.1	982	27.9	936	25	11	a″	817	7.7	835	2.6		
12	a$_1$	1052	0.5	1052	0.7			12	a″	882	0.7	929	0.4		
13	a$_1$	1118	0.4	1107	0.9			13	a′	889	35.6	910	16.6	877.0	w
14	b$_2$	1152	0.2	1141	0.1			14	a′	1008	11.4	1015	16.9	971.0	w
15	b$_2$	1284	0.5	1268	0.0			15	a′	1134	2.5	1122	4.8	1128.6	vw
16	b$_2$	1336	0.4	1320	0.0			16	a′	1195	116.9	1178	134.3	1157.6	m
17	b$_2$	1420	0.0	1410	0.0			17	a′	1275	97.7	1266	84.5	1209.1	m
18	a$_1$	1454	14.9	1432	16.1	1402	15	18	a′	1317	42.0	1310	28.6	1254.9	m
19	b$_2$	1544	18.6	1531	8.0	1486	15	19	a′	1336	4.8	1320	6.1	1290.1	w
20	a$_1$	1706	3.9	1687	3.9			20	a′	1426	64.9	1418	42.5	1368.2	m
21	a$_1$	3210	22.8	3159	21.6			21	a′	1475	15.4	1448	15.1	1429.0	w
22	b$_2$	3251	12.6	3195	8.7			22	a′	1589	118.5	1564	108.2	1516.3	s
23	a$_1$	3256	7.4	3200	7.3			23	a′	1703	15.4	1678	27.5		
24	a$_1$	3289	4.9	3225	3.4	3037	5	24	a′	3232	11.2	3180	10.4		
								25	a′	3254	8.3	3200	6.1		
								26	a′	3295	3.9	3228	2.7		
								27	a′	3880	51.7	3817	51.4	3612.0	m

[a] Frequencies ω in cm^{-1}, intensities I in km/mol. In the case of the experimental data relative intensities are given. The experimental spectra were measured only above 500 cm^{-1}.

In Figure 3, the infrared spectrum of **9a**, calculated at the CCSD(T)/6-31G(d,p) level of theory, is compared to the corresponding measured infrared spectrum. In Table 4, CCSD-(T) frequency and intensity values are given for all vibrational modes of **1** and **9a**. A characterization of these modes including phenol as a suitable reference molecule is given in Table 5, where the adiabatic mode analysis of Konkoli and Cremer[27] has been used to carry out correlation and characterization of calculated normal modes. Since a CCSD(T) calculation of the vibrational spectrum of phenol is not feasible, the analysis is based on the B3LYP/6-31G(d,p) data. Table 4 reveals that this is justified considering the similarity of the CCSD(T) and B3LYP description of the vibrational modes.

For both **1** and **9a** there is convincing agreement between measured and calculated (CCSD(T) and B3LYP) infrared spectra, while HF, MP2, and GVB lead to infrared spectra that strongly differ from the CCSD(T) and the experimental spectra. Reliable calculations on *m*-benzynes are problematic because of their multireference character. Accordingly, HF and low-order MP perturbation theory fail in this case while a two-configuration approach, e.g., GVB leads to a reasonable description of the *m*-benzyne wave function but, however, lacks needed dynamic electron correlation. Both CCSD(T) and DFT cover high-order dynamic electron correlation effects and, by this, also some of the multireference effects. Because of this and because of the reduced biradical character of *m*-benzynes (20−40% according to different ways of calculating the biradical character),[26] both CCSD(T) and B3LYP lead to reliable descriptions of energetic, structural, and spectroscopic properties of *m*-benzynes.

The most intense infrared band of **1** (at 547 cm^{-1}) corresponds to a b$_2$-symmetrical ring deformation mode that causes CCC bending at C1 and C4 and (out of phase) at C2 and C5 (Table 5). Since this motion implies opposing rehybridization effects at the radical centers, it is sensitive to a correct description of electron correlation. For example, GVB seriously overestimates the harmonic frequency and underestimates the intensity of this mode. The other infrared bands measured correspond to b$_1$-symmetrical H out-of-plane bendings (CH wagging motions no. 6 and no. 7 at 751 and 824 cm^{-1}), a b$_2$-symmetrical CC stretching (and partially HCC bending) motion at 936 cm^{-1} (no. 11), and a$_1$- and b$_2$-symmetrical modes at 1402 (no. 18) and 1486 cm^{-1} (no. 19) with character similar to that of mode no. 11 (Table 5).

Hence, **1** can best be recognized by the very strong ring deformation band at 547 cm^{-1} and the half as intense CH wagging band at 751 cm^{-1}. These two bands can be used to distinguish benzene, *o*-benzyne, **1**, and *p*-benzyne by their infrared spectra. For benzene, the CH wagging band is very strong (671 cm^{-1}),[28,29] while the ring deformation mode has zero intensity because of symmetry reasons. For *o*-benzyne, the intensities for the two vibrational modes are similar as found for **1**, but the ring deformation mode is found below 500 at 472 cm^{-1}.[30,2] CCSD(T) and DFT calculations for *p*-benzyne suggest that the ring deformation band is only of medium and the CH wagging motion again of very strong intensity.[31]

OH substitution results in splitting of the ring deformation mode at 547 cm^{-1} into two less intense bands at 519 and 641 cm^{-1}. The CH wagging band in **9a** (at 695 cm^{-1}) is again of lower intensity than the ring deformation modes. The calculations suggest that the OH torsion band (no. 2, not measured), the COH bending band (no. 16, 1158 cm^{-1}) and the CC stretching/HCC bending band corresponding to band no. 19 of

(27) (a) Konkoli, Z; Cremer, D. *Int. J. Quantum Chem.*, submitted. (b) Konkoli, Z.; Larsson, A.; Cremer, D. *Int. J. Quantum Chem.*, submitted.

(28) Varsanyi, G. *Vibrational Spectra of Benzene Derivatives*; Academic Press: New York; London, 1969.

(29) Brown, K. G.; Person, W. B. *Spectrochim. Acta* **1978**, *34A*, 117−122.

(30) Simon, J. G. G .; Münzel, N.; Schweig, A. *Chem. Phys. Lett.* **1990**, *170*, 187−192.

(31) Bochum and Göteborg et al. To be published.

Table 5.   Characterization and Correlation of the Normal Modes of Phenol, 2,4-Dehydrophenol (**9a**), and *m*-Benzyne (**1**)

phenol, C_s symmetry			9a, C_s symmetry		1, C_{2v} symmetry		
mode	sym	character	mode	character	mode	sym	character
1	a″	79% ring (boat)	4	66% ring torsion	2	b₁	91% ring torsion (boat)
2	a″	96% OH torsion	3	73% OH torsion			
3	a′	69% CCO bend	5	47% COH bend, 24% CCC bend	13	a₁	49% HCC bend, 17% CC stretch
4	a″	72% ring (twistboat)	6	73% ring torsion (twistboat)	3	a₂	60% ring torsion (twistboat)
5	a″	29% O oop bend, 43% ring torsion	8	25% O oop bend, 53% ring torsion	8	a₂	93% H oop bend
6	a′	70% CCC bend	2	86% CCC bend	1	a₁	89% CCC bend
7	a′	92% CCC bend	7	85% CCC bend	4	b₂	92% CCC bend
8	a″	74% ring (chair)	1	84% ring torsion (halfchair)	5	b₁	90% ring torsion (chair)
9	a″	36% H oop, 11% O oop bend					
10	a″	88.5 H oop bend					
11	a′	53% CCC bend, 18% CO, 20% CC stretch	9	59% CCC bend, 15% CO stretch	9	a₁	86% CCC bend
12	a″	77% H oop bend	13	82% H oop bend	10	b₁	83% H oop bend
13	a″	84% H oop bend	10	84% H oop bend	6	b₁	81% H oop bend
14	a″	88% H oop bend	11	87% H oop bend	7	b₁	85% H oop bend
15	a′	80% CCC bend	12	44% CCC bend, 38% CC stretch	12	a₁	66% CC stretch, 24% HCC bend
16	a′	50% CC stretch	14	71% CC stretch, 12% HCC bend	11	b₂	66% CC stretch, 10% HCC bend
17	a′	32% CCH bend, 29% CC stretch	15	65% HCC bend, 15% CC stretch	14	b₂	75 HCC bend
18	a′	75% HCC bend					
19	a′	78% HCC bend					
20	a′	50% COH bend, 13% CC stretch	16	41% COH bend, 22 CC stretch, 14% HCC			
21	a′	47% CO stretch	18	37% CO stretch, 21% HCC, 14% CC stretch	22	b₂	99% CH stretch
22	a′	42% HCC bend, 37% CC stretch	21	41% CC stretch, 22% COH, 12% HCC	17	b₂	73% CC stretch
23	a′	45% HCC bend	17	56% HCC bend, 16% CO stretch, 13% COH	15	b₂	75% HCC bend
24	a′	47% HCC bend, 24% CC stretch	19	57% CC stretch, 25% HCC bend	16	b₂	42% CC stretch, 41% HCC bend
25	a′	43% HCC bend, 29% CC stretch	20	55% CC stretch, 20% HCC, 22% COH	18	a₁	51% HCC bend, 29% CC stretch
26	a′	42% CC stretch	23	78% CC stretch	20	a₁	85% CC stretch
27	a′	59% CC stretch	22	41% CC stretch, 19% HCC	19	b₂	34% CC stretch, 29% HCC bend
28	a′	90% CH stretch					
29	a′	91% CH stretch	25	99% CH stretch	23	a₁	90% CH stretch
30	a′	86% CH stretch	26	99% CH stretch	24	a₁	99% CH stretch
31	a′	97% CH stretch					
32	a′	96% CH stretch	24	99% CH stretch	21	a₁	90% CH stretch
33	a′	100% OH stretch	27	100% OH stretch			

a According to B3LYP/6-31G(d,p) calculations.

1 (no. 22, 1516 cm $^{-1}$) should be of higher intensity, which is only partially confirmed by the experiment. The best agreement between experiment and theory is obtained when scaling factors of 0.979 (CCSD(T)) and 0.970 (B3LYP) are used in the case of **1**, and 0.955 (0.954), in the case of **9a**. As can be seen from Figure 3, the agreement between CCSD(T) and experimental infrared spectra clearly confirms that **9a** has been isolated in the matrix and that the geometry is described best as σ-biradical (Figure 8).

Although the bicyclic isomers **2** and **10a** are not observed under the conditions of matrix isolation, it is of general interest to calculate the infrared spectra of the bicyclic forms. **2** and **10a** are stationary points at the B3LYP/6-31G(d,p) but not at the CCSD(T)/6-31G(d,p) level of theory. The best way of identifying the bicyclic isomer of a *m*-benzyne is to look for the CC stretching motion of the three-membered ring, which should occur close to 1800 cm^{-1} (B3LYP, 1854; scaled with 0.96, 1780 cm^{-1}). This band is weak but should be detectable, since there are no other overlapping absorptions in this region. Apart from this, the infrared spectra of the closed-shell structures **2** and **10a** differ significantly from those of the diradicals **1** and **9a**.

In principle, the vibrational frequencies and intensities of a molecule contain important information on the electronic structure. However, the vibrational normal modes of a molecule are delocalized modes and the electronic structure information is encoded in a complicated way. A powerful way to unravel this information is the adiabatic mode analysis of Konkoli and Cremer,[27] which is based on localized adiabatic internal modes that are associated with the internal coordinates used to define the geometry of a molecule. Once the normal modes of a molecule are known, the calculation of the corresponding adiabatic modes is straightforward.

In Table 3 for selected geometrical parameters the corresponding B3LYP adiabatic frequencies are given. In most cases, adiabatic frequencies of stretching modes are inversely proportional to the corresponding lengths, i.e., shorter bond lengths lead to larger adiabatic frequencies and vice versa.[32] For example, the calculated CC bond lengths of phenol (Table 3) correlate linearly with the corresponding adiabatic frequencies. However, adiabatic stretching frequencies depend not only on the bond length but also on the environment of a bond as, e.g., the type of atoms, groups or substituents attached to the bond in question, or the steric arrangement of neighboring bonds. Thus, the adiabatic stretching frequencies are more appropriate than bond lengths to reflect the strength of a bond, which depends on the electron density between the bonded atoms as well as on environmental effects.

The adiabatic stretching frequencies of **1** and **9a** reveal that despite the CC bond length shortening the ring bonds are not necessarily more stable. On the contrary, in some cases, the adiabatic frequencies are smaller than in the reference molecule

(32) Larsson, A.; Cremer, D. To be published.

phenol. Also, they indicate a strengthening of bonds C1C2 and C4C5 relative to the other ring bonds, which confirms the importance of through-bond stabilization effects. However, in total, the carbon ring is less stiff than in phenol, which is particularly reflected by the much smaller adiabatic CCC bending and CCCC torsional frequencies. Both in-plane and out-of-plane distortions of the six-membered ring should easier occur in the case of **1** and **9a** than either benzene or phenol.

Discussion

It has been shown that the photodecarboxylation of 4-oxo-cyclohexadienylidene-3-carboxylic acids (**8**), which is a special type of the decarboxylation reaction of β-keto acids, yields 2,4-didehydrophenols (**9**) smoothly and in high quantum yield. The formation of **9** from **7** is a biphotonic process with loss of N_2 with carbene **8** as the primary intermediate followed by decarboxylation on $\lambda > 470$ nm irradiation as the second step. Interestingly, the highly photolabile carbenes **8** can be cleanly prepared under the conditions of matrix isolation by monochromatic irradiation of **7** with blue light.
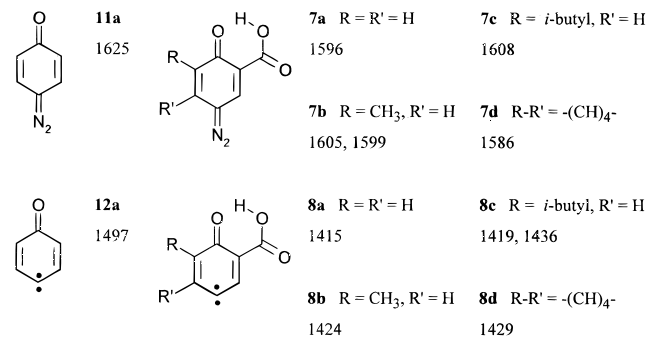
The thermodynamic driving force for this reaction is the formation of carbon dioxide: the heat of formation of **9a** is 85 kcal/mol (see previous section) so that the sums of the heats of formation of **9a** and CO_2 is -9 kcal/mol. The heat of formation of triplet carbene **8a** can be estimated from Benson's group increments[33] to be 9 kcal/mol. Hence, the reaction **8a** $\rightarrow$ **9a** + CO_2 is exothermic by 18 kcal mol^{-1}.

Nevertheless, it has to be discussed why this reaction proceeds so readily. Usually, the hydroxy protons of carboxylic acids are very firmly bound and hard to abstract. The observation that intramolecular hydrogen abstraction takes place by the keto oxygen atom, which is a radical site that bears only partial phenoxy character (and should thus not have a particularly high free radical reactivity), indicates that the O–H bond of the carboxylic acid moiety of carbene **8a** has to be already significantly weakened. The clue to the problem comes from the X-ray structure analysis of diazo compounds **7a,c**.[16] The structures clearly reveal the presence of an intramolecular hydrogen bridge. Of particular interest are the extremely short distances between the keto- and OH-carboxy oxygen atoms with 2.475 Å in **7a** and even less (2.442 Å) in **7c**. The O–O distances in O–H–O hydrogen bridges have been correlated with the strength of the hydrogen bridge;[34] thus, the hydrogen bridges observed in **7a,c** can be counted among the strongest hydrogen bridges known.

This is confirmed by the proton NMR spectra of **7**, where the O–H protons give sharp resonances between $\delta = 11$ and 17, and by the ^{13}C NMR spectra. The chemical shift of the diazo carbon (C4) of **7a** is found at $\delta = 87.0$ (in DMSO-d_6), while the corresponding shift of *p*-benzoquinone diazide **11a** is $\delta = 73.6$ (in CDCl$_3$). Since the value for δ (C1) of the benzene diazonium ion is around $\delta = 109.7$ (as chloride),[35] it is clear that the quinone diazide carboxylic acids (**7**) range approximately halfway between typical quinone diazides and highly polar intramolecular diazonium–phenolate ion pairs.

Further evidence for strong intramolecular hydrogen bonding can be found in the infrared spectra of **7**. Due to the strong O–H–O bridges, the intensities of the OH stretching vibrations are very low and generally not to be detected in the spectra, while free carboxylic acids exhibit strong OH stretching

(33) Benson, S. W.; Cruickshank, F. R.; Golden, D. M.; Haugen, G. R.; O'Neal, H. E.; Rodgers, A. S.; Shaw, R.; Walsh, R. *Chem. Rev.* **1969**, *69*, 279–324.

(34) Ichikawa, M. *Acta Crystallogr.* **1978**, *B34*, 2074–2080.

(35) Duthaler, R. O.; Foerster, H. G.; Roberts, J. D. *J. Am. Chem. Soc.* **1978**, *100*, 4974–4979.

Scheme 4

11a 1625	**7a** R = R' = H 1596	**7c** R = *i*-butyl, R' = H 1608
	7b R = CH$_3$, R' = H 1605, 1599	**7d** R-R' = -(CH)$_4$- 1586
12a 1497	**8a** R = R' = H 1415	**8c** R = *i*-butyl, R' = H 1419, 1436
	8b R = CH$_3$, R' = H 1424	**8d** R-R' = -(CH)$_4$- 1429

vibrations that can be easily recognized by matrix isolation spectroscopy (cf. ketene **19**). The hydrogen bridge results in a significant lowering of the carbonyl bond order. Consequently, the CO stretching frequency in **7a** is red-shifted by 29 cm^{-1} compared to quinone diazide **11a** (Scheme 4).[16,14] Concurrently, the NN stretching vibration of **7a** at 2114 cm^{-1} is red-shifted by almost 38 cm^{-1} compared to **11a**. These infrared shifts, which are similarly also observed in **7b**–**d**, indicate that the introduction of an intramolecular hydrogen bridge augments the weight of the diazonium phenolate mesomeric structure of **7**.

While the tools of X-ray structure analysis and proton NMR spectroscopy are not available for the determination of the structures of the corresponding carbenes **8**, the IR spectra clearly indicate very strong hydrogen bridges, which might even exaggerate that of **7**. Again, the intensity of the OH stretching vibrations in **8** are very low and not to be detected in the spectra. The carbonyl stretching vibration of carbene **8a** is found at 1415
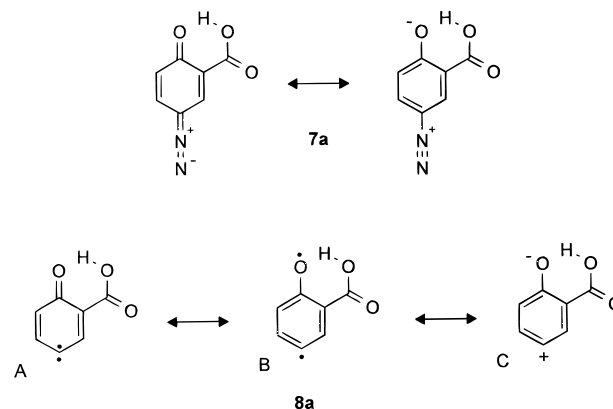
cm^{-1} and thus red-shifted by 82 cm^{-1} compared to **12a** (Scheme 4). This clearly demonstrates the importance of the diradicaloid and zwitterionic resonance structures B and C, respectively, to describe the wave function of **8a**. The zwitterionic resonance structure C is also in line with the phenyl cation type reactivity in slightly acidic solvents such as trifluoroethanol.

It is not clear from our experiments if the decarboxylation of carbenes **8** is a photochemical or a hot ground-state reaction and at which point along the reaction coordinate the intersystem crossing from the triplet (carbene) to the singlet surface (*m*-benzyne) occurs. A strong hydrogen bridge was observed in all diazo compounds **7**, carbenes **8**, carbonyl oxides **13**, and dioxiranes **14** with quite different substituents at the six-membered ring. Even if in a reactive excited state of **8** the charge at the carbonyl oxygen atom might be reduced compared to the triplet ground state, it is reasonable to assume that there is still a strong hydrogen bond. In any case, the transfer of the hydrogen atom is facilitated by the very strong O–H–O hydrogen bridge. The decarboxylation might occur concerted with the hydrogen migration or in a second step. In an acidic solvent, where the carbonyl oxygen atom is already protonated

Scheme 5
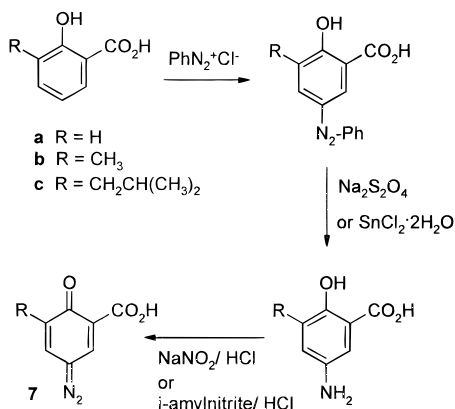
and thus proton transfer from the carboxylic group cannot occur, no decarboxylation is observed. This clearly demonstrates that proton transfer and decarboxylation are linked together.

In summary, quinone diazide carbocylic acids (**7**) provide interesting precursors of 2,4-didehydrophenols (**9**), a novel class of *m*-benzynes. Since the diazo compounds are readily synthesized via standard procedures, a variety of substitution patterns are easily accessible. Due to the highly polar character and strong packing forces in the crystals of **7a**, the solubility of this diazo compound in common solvents is very low. However, by introducing alkyl substituents, the solubility increases and the solution chemistry can be conveniently studied. Carbenes **8** as well as the *m*-benzynes **9** were unequivocally characterized using matrix isolation spectroscopy and by trapping experiments in solution. Detailed insight into the spectroscopic properties and electronic structure of **9a** is provided by ab initio calculations at the CCSD(T) level of theory in combination with the infrared spectra.

Experimental Section

Materials and General Methods. The NMR spectra were recorded with a Bruker AM-400 spectrometer, and chemical shifts are reported in parts per million (δ) relative to TMS unless otherwise indicated. Gas chromatography (GC) was performed by the use of a Siemens Sichromat equipped with glass capillary columns (39 m, OV17, 160 °C). High-pressure liquid chromatography with LCD (Milton Roy) chromatographs and refractometric detection. Mass spectra were obtained on Varian MAT CH5 instrument (70 eV). Melting points were determined on a Kofler hot-stage apparatus and are uncorrected. Acetonitrile and tetrachloromethane (for UV spectroscopy) were obtained from Acros Chimica, while MTHF was distilled immediately prior to use. For product analysis, dilute degassed solutions of the diazo compounds were irradiated.

3-Diazo-6-oxo-1,4-cyclohexadiene-1-carboxylic acid (**8a**)[10,36] and its 3-alkylated derivatives **7b−d** were synthesized by diazotization of the corresponding 5-aminosalicylic acids according to the procedure of Ried and Appel (Scheme 5).[37] Purification of the diazo compounds was accomplished by recrystallization from water/acetone (1:1).

Diazo compounds **7** were deuterated at the carboxy position by briefly heating the compounds to ~70 °C in a 1:1 mixture of acetonitrile and D$_2$O. The degree of deuteration obtained was never in excess of 80%. Attempts to drive the exchange reaction to completion by longer reaction times or higher temperatures failed due to competing decomposition of the diazo compounds.

1,4-Naphthoquinone Diazide 2-Carboxylic Acid (7d). 4-Amino-1-hydroxy-2-naphthoic acid[38] was dissolved in ethanol, saturated with gaseous HCl. After being cooled to 5 °C, the mixture was treated with a small excess of isoamylnitrite. The reaction mixture was then stirred for 1 h and subsequently poured into diethyl ether and cooled to −10 °C. The diazide precipitated after a while and was recrystallized from

acetone/ water (1:1): yellow needles; mp 182 °C (dec); ^{1}H NMR (DMSO-d_6) δ 15.24 (s, br, 1H), 9.28 (s, 1H), 8.42 (d, 1H, ^3J = 8.6 Hz), 7.88 (m, 2H), 7.67 (m, 1H); ^{13}C NMR (DMSO-d_6) δ 81.0, 114.1, 121.8, 126.6, 127.1, 128.5, 129.4, 132.8, 142.5, 165.2, 180.0; IR (KBr) 3432 (w), 3087 (w), 2159 (s, N≡N), 1717 (s), 1613 (m), 1578 (s), 1540 (s), 1506 (s), 1476 (s), 1408 (m), 1363 (w), 1319 (w), 1291 (m), 1266 (w), 1198 (s), 1168 (s), 1050 (w), 941 (w), 810 (vw), 763 (s) cm^{-1}; HRMS calcd for C$_{11}$H$_6$N$_2$O$_3$ 214.0378, found 214.0377; MS *m/z* (relative intensity) 214 (4, M$^+$), 186 (14), 170 (27), 158 (15), 142 (7), 114 (39), 102 (10), 88 (9), 71 (7), 63 (12), 57 (7), 50 (5), 44 (27), 39 (7), 28 (100). Anal. Calcd for C$_{11}$H$_6$N$_2$O$_3$ C, 61.73; H, 2.82, found C, 61.82; H, 2.78.

4-Amino-3-hydroxy-2-naphthoic Acid was synthesized by azo coupling of benzenediazonium chloride with 3-hydroxy-2-naphthoic acid followed by reduction of the azo compound with Na$_2$S$_2$O$_4$.

1,2-Naphthoquinone 1-Diazide 3-Carboxylic Acid (18). 4-Amino-3-hydroxy-2-naphthoic acid was dissolved in ethanol, saturated with gaseous HCl. After being cooled to 5 °C, the mixture was treated with a small excess of isoamylnitrite. The reaction mixture was stirred for 1 h, poured into diethyl ether, and cooled. The diazide precipitated after a while and was recrystallized from acetone/water (1:1): yellow needles; mp 182 °C (182 °C); ^{1}H NMR (DMSO-d_6) δ 10.6 (s, broad, 1H), 8.8 (s, 1H), 8.16−8.06 (m, 1H), 7.82−7.76 (m, 2H), 7.6−7.1 (m, 1H); ^{13}C NMR (DMSO-d_6) δ 178.2, 165.0, 145.9, 132.9, 132.4, 129.1, 125.3, 122.9, 121.5, 120.6, 83.2; IR (KBr) 3034 (m), 2140 (vs), 1717 (vs), 1612 (vs), 1581 (vs), 1552 (vs), 1491 (vs), 1459 (vs), 1384 (vs), 1352 (vs), 1276 (s), 1215 (vs), 1166 (s), 1087 (m), 883 (m), 799 (m), 763 (m) cm^{-1}; MS *m/z* (relative intensity) 214 (M$^+$, 47), 186 (84), 169 (23), 142 (52), 130 (20), 114 (54), 102 (100), 87 (25), 76 (17), 71 (12), 63 (47), 57 (11), 51 (14), 39 (20), 28 (38);

Matrix Isolation. Matrix isolation experiments were performed by standard techniques with an APD CSW-202 Displex closed-cycle helium cryostat.[39] Matrices were produced by deposition of argon (Linde, 99.9999%) on top of CsI (IR) or sapphire (UV−vis) window with a rate of approximately 0.15 mmol/min. Infrared spectra were recorded by using a Bruker IFS66 FTIR spectrometer with a standard resolution of 1 cm^{-1} in the range 400−4000 cm^{-1}. UV−vis spectra were recorded on a Hewlett-Packard 8452A diode array spectrophotometer with a resolution of 2 nm. Irradiations were carried out with use of Ushio HBO 500 W mercury high-pressure arc lamps in Oriel housings equipped with quartz optics. IR irradiation from the lamps was absorbed by a 10 cm path of water. For broad-band irradiation, Schott cutoff filters were used (50% transmission at the wavelength specified), and for narrow-band irradiation, interference filters in combination with dichroic mirrors ("cold mirrors") and cutoff filters were used.

4-Diazo-1-oxo-2,5-cyclohexadiene-2-carboxylic Acid (7a): IR (Ar, 10 K) 2113.6 (s), 2092.9 (w), 2057.2 (vw), 1740.9 (w), 1595.8 (vs), 1564.0 (vw), 1535.1 (w), 1481.1 (m), 1473.3 (s), 1458.4 (w), 1379.3 (w), 1335.0 (vw), 1260.3 (vw), 1204.3 (vw), 1164.8 (s), 1127.2 (w), 838.9 (vw), 528.9 (vw) cm^{-1}(relative intensity); temperature of deposition 136 °C.

1-Oxo-2,5-Cyclohexadien-4-ylidene-2-carboxylic Acid (8a): IR (Ar, 10 K) 1758.3 (vs, 0.994), 1750.1 (m, -), 1523.5 (w, -), 1495.0 (m, 0.998), 1458.9 (w, 0.999), 1422.2 (s, −), 1415.0 (vs, 1.000), 1383.7 (w, 1.000), 1291.6 (w, 1.001), 1228.9 (w, −), 1053.9 (vw, −), 982.6 (vw, −), 826.3 (w, −), 565.0 (vw, 1.000), 542.9 (vw, −) cm^{-1} (relative intensity, ratio of ^{2}H/^{1}H isotopic frequencies ν_i/ν).

2,4-Didehydrophenol (9a): IR (Ar, 10 K) 3612.0 (s, 0.738), 1516.3 (s, 0.997), 1429.0 (w, 0.982), 1368.2 (m, 0.987), 1290.1 (w, 0.979), 1254.9 (m, −), 1209.1 (m, −), 1157.6 (m, 0.814), 1128.6 (vw, −), 971.0 (w, 1.008), 877.0 (w, 0.997), 694.7 (m, 0.981), 641.2 (s, 1.000), 518.8 (s, 0.984) cm^{-1} (relative intensity, ratio of ^{2}H/ ^{1}H isotopic frequencies ν_i/ν).

1,4-Benzoquinone-2-carboxylic Acid 4-*O*-Oxide (13a): IR (Ar, 10K) 1774.2 (m, 0.998), 1764.5 (vs, 1.000), 1753.3 (s, 1.000), 1607.9 (vs, 1.000), 1577.0 (s, 0.999), 1573.1 (s, 0.998), 1416.5 (vs, 1.000), 1408.3 (s, 1.001), 1382.2 (w, 0.999), 1351.4 (w, 1.001), 1343.7 (w, 0.999), 1235.2 (m, 0.999), 1222.6 (s, 0.998), 1218.8 (m, −), 1176.4 (m, 0.996), 1101.6 (s, 0.984), 1069.3 (m, 0.968), 1066.0 (m, 0.960), 1003.8 (m, 0.988), 943.0 (m, 0.999), 932.4 (vw, −), 890.5 (w, 1.001), 886.1 (w, 0.998), 880.3 (w, 1.001), 823.5 (vw, 1.001), 819.6 (vw,

(36) Rugeddi, A. *Gazz. Chim. Ital.* **1929**, 13.
(37) Ried, W.; Appel, H. *Liebigs Ann. Chem.* **1961**, *646*, 82−95.
(38) Grandmougin, E. *Chem. Ber.* **1906**, *39*, 3609−3611.

(39) Sander, W. W. *J. Org. Chem.* **1989**, *54*, 333−339.

0.999), 813.3 (w, 0.999), 723.2 (w, 1.001), 708.2 (w, 0.990), 655.2 (w, −), 594.4 (w, −), 585.3 (w, 1.001) cm⁻¹ (relative intensity, ratio of ¹⁸O/¹⁶O isotopic frequencies ν_i/ν).

6-Oxo-1,2-Dioxaspiro[2,5]octa-4,7-diene-5-carboxylic   Acid (14a): IR (Ar, 10K) 1778.0 (vs, 1.000), 1674.9 (s, 0.998), 1657.0 (s, 0.995), 1633.4 (w, 1.001), 1405.9 (vs, 0.996), 1395.2 (vs, 1.000), 1391.9 (vs, −), 1321.5 (m, 0.998), 1271.3 (vw, 0.994), 1105.0 (m, 1.000), 1039.0 (m, −), 1034.1 (m, 0.995), 989.3 (vw, 0.992), 953.1 (vw, 0.995), 864.0 (w, 0.995), 853.3 (m, 1.001), 847.6 (m, 0.999), 804.2 (w, 0.990), 793.1 (w, 0.998), 654.2 (m, −) cm⁻¹ (relative intensity, ratio of ¹⁸O/¹⁶O isotopic frequencies ν_i/ν).

6-Methyl-4-diazo-1-oxo-2,5-cyclohexadiene-2-carboxylic   Acid (7b): IR (Ar, 10K) 2181.7 (11), 2213 (14), 2175.8 (15), 2129 (41), 2121.6 (38), 2116.6 (44), 2103.8 (100), 2098.8 (82), 2080.5 (12), 2073.6 (16), 1742.1 (48), 1728.4 (28), 1618.1 (26), 1605.3 (72), 1599.4 (64), 1564.6 (78), 1536.3 (15), 1492.8 (39), 1478.2 (50), 1459.5 (44), 1433.8 (29), 1382.2 (14), 1358.8 (42), 1240.9 (23), 1227.1 (71), 1182.8 (30), 1176.8 (71), 1106.9 (55), 1010.4 (11), 952.3 (10), 926.2 (4), 899.1 (−), 666.2 (−), 536.6 (−) cm⁻¹ (relative intensity). Temperature of deposition 140 °C.

6-Methyl-1-oxo-2,5-cyclohexadien-4-ylidene-2-carboxylic   Acid (8b): IR (Ar, 10K) 1764.6 (73, 0.999), 1757.4 (100, 0.999), 1520.7 (13, 1.000), 1504.8 (33, 0.996), 1424.9 (78, 0.996), 1417.6 (50, 0.990), 1399.1 (49, 0.996), 1374.5 (21, 1.000), 1326.5 (vw, −), 1288.7 (34, 0.988), 1136.2 (26, 0.954), 1023.8 (w, 0.999), 851.5 (w, 1.004), 790.5 (w, −), 724.0 (w, −), 598.0 (w, −) cm⁻¹ (relative intensity, ratio of ²H/¹H isotopic frequencies ν_i/ν).

6-Methyl-2,4-didehydrophenol (9b): IR (Ar, 10K) 3612.3 (100, 0.738), 1500.9 (37, 0.996), 1377.0 (34, −), 1262.6 (12, 0.993), 1249.2 (38, 0.996), 1242.9 (30, 0.742), 1204.7 (22, 0.993), 1063.0 (11, 0.995), 1039.3 (2, 0.999), 1015.3 (16, 1.000), 944.1 (18, 0.999), 731.7 (14, 0.977), 662.1 (24, 1.004), 641.3 (22, 0.999), 620.9 (4, 1.000), 509.8 (w, 1.000) cm⁻¹ (relative intensity, ratio of ²H/¹H isotopic frequencies ν_i/ν).

6-Methyl-1,4-benzoquinone-2-carboxylic Acid 4-O-Oxide (13b): IR (Ar, 10 K) 1774.2 (m, 0.998), 1764.5 (vs, 1.000), 1753.3 (s, 1.000), 1607.9 (vs, 1.000), 1577.0 (s, 0.999), 1573.1 (s, 0.998), 1416.5 (vs, 1.000), 1408.3 (s, 1.001), 1382.2 (w, 0.999), 1351.4 (w, 1.001), 1343.7 (w, 0.999), 1235.2 (m, 0.999), 1222.6 (s, 0.998), 1218.8 (m, −), 1176.4 (m, 0.996), 1101.6 (s, 0.984), 1069.3 (m, 0.968), 1066.0 (m, 0.960), 1003.8 (m, 0.988), 943.0 (m, 0.999), 932.4 (vw, −), 890.5 (w, 1.001), 886.1 (w, 0.998), 880.3 (w, 1.000), 823.5 (vw, 1.001), 819.6 (vw, 0.999), 813.3 (w, 0.999), 723.2 (w, 1.001), 708.2 (w, 0.990), 655.2 (w, −), 594.4 (w, −), 585.3 (w, 1.001) cm⁻¹ (relative intensity, ratio of ¹⁸O/¹⁶O isotopic frequencies ν_i/ν).

1,2-Dioxa-7-methyl-6-oxospiro[2,5]octa-4,7-diene-5-carboxylic Acid (14b): IR (Ar, 10 K) 1783.8 (s, −), 1779.0 (vs, 1.001), 1769.8 (m, −), 1674.4 (m, 1.001), 1669.1 (m, −), 1657.5 (m, 1.000), 1645.5 (m, 0.999), 1448.3 (w, 1.000), 1394.3 (vs, 0.999), 1387.0 (s, −), 1358.1 (vw, −), 1354.7 (vw, 0.995), 1317.6 (m, 0.999), 1294.5 (w, 1.001), 1249.2 (vw, 1.000), 1241.9 (vw, 1.000), 1120.0 (vw, 1.000), 1039.4 (vw, 1.000), 1031.2 (vw, −), 1014.9 (w, 0.999), 950.3 (vw, 0.994), 926.2 (vw, 0.999), 872.6 (vw, −), 810.4 (vw, −), 798.9 (m, 0.998), 770.9 (vw, 1.000), 731.4 (vw, 1.000), 690.9 (vw, 0.997), 674.5 (vw, 0.993), 660.5 (w, 1.000), 642.2 (w, 1.000), 510.1 (vw, 0.998) cm⁻¹ (relative intensity, ratio of ¹⁸O/¹⁶O isotopic frequencies ν_i/ν).

6-Isobutyl-4-diazo-1-oxo-2,5-cyclohexadiene-2-carboxylic Acid (7c): IR (Ar, 10K) 2105.6 (m), 1742.4 (m), 1607.9 (m), 1561.4 (w), 1479.0 (w), 1461.0 (vw), 1289.1 (vw), 1176.6 (w), 1126 (vw), 1113 (vw) cm⁻¹ (relative intensity); temperature of deposition 112 °C.

6-Isobutyl-1-oxo-2,5-cyclohexadien-4-ylidene-2-carboxylic Acid (8c): IR (Ar, 10K) 1760.5 (s), 1717.4 (m), 1699 (vw), 1695.7 (w), 1684.6 (w), 1652.5 (w), 1616.4 (w), 1576.0 (m), 1495.7 (vw), 1436.2 (vw), 1419.1 (vw) cm⁻¹ (relative intensity).

6-Isobutyl-2,4-didehydrophenol (9c): IR (Ar, 10K) 3612.5 (vs), 1595 (w), 1493 (m), 1289.0 (m), 1246.4 (s), 1092 (m), 667.4 (m), 659 (m), 641 (m) cm⁻¹ (relative intensity).

1,4-Naphthoquinone 4-Diazo 2-Carboxylic Acid (7d): IR (Ar, 10K) 2134.1 (m), 2105.1 (s), 2086.5 (s), 2073.3 (w), 1762 (s), 1731.9 (m), 1616.8 (m), 1608.2 (s), 1585.9 (vs), 1551.6 (s), 1543.7 (w), 1477.9 (m), 1462.2 (m), 1456.8 (m), 1452.3 (s), 1448.4 (s), 1295.7 (s), 1266.6

(m), 1211.6 (m), 1196.4 (vs), 1166.3 (m), 762.4 (m), 759.0 (w), 612.8 (w), 495.2 (vw) cm⁻¹ (relative intensity); temperature of deposition 155 °C.

1,4-Dihydro-1-oxonaphthalen-4-ylidene-2-carboxylic Acid (8d): IR (Ar, 10K) 1753.0 (s), 1744.6 (m), 1716.9 (w), 1561.2 (m), 1558.3 (m), 1540.2 (m), 1470.9 (m), 1441 (m), 1429.3 (vs), 1405.8 (m), 1397.3 (s), 1325.4 (w), 1305.7 (vw), 1273.8 (w), 1140.9 (w), 901.0 (vw), 737.6 (vw), 724.5 (vw), 640.5 (w), 476.3 (w) cm⁻¹ (relative intensity). **2,4-Didehydro-1-naphthol (9d)**: IR (Ar, 10K) 3608 (s), 1604.6 (m), 1582.5 (w), 1546.0 (vw), 1485.1 (vw), 1453.9 (vw), 1392.1 (w), 1343.0 (w), 1336.2 (w), 1334.4 (w), 1236.1 (w), 1233.2 (w), 1216.4 (vw), 1212.3 (vw), 1167.8 (m), 1011.0 (vw), 981.5 (m), 976.8 (m), 788.8 (m), 758.5 (m), 659.9 (w), 645.7 (vw), 641.6 (vw), 639.0 (vw), 631.0 (vw), 603 (vw) cm⁻¹ (relative intensity).

1,2-Naphthoquinone 2-Diazide 3-Carboxylic Acid (18): IR (Ar, 10K) 2120 (79), 2117 (5), 2103 (19), 1768 (1), 1767 (69), 1762 (14), 1670 (5), 1620 (100), 1611 (13), 1606 (2), 1600 (22), 1566 (88), 1487 (18), 1462 (55), 1443 (2), 1438 (8), 1377 (15), 1375 (4), 1299 (6), 1295 (2), 1289 (4), 1277 (19), 1215 (19), 1209 (76), 1203 (15), 1193 (5), 1163 (15), 1093 (6), 1017 (2), 967 (4), 857 (11), 800 (19), 757 (5), 749 (16), 701 (4), 665 (9), 590 (8), 492 (6), 454 (6) cm⁻¹ (relative intensity); temperature of deposition 140 °C.

1-Carbonyl-1H-indene-2-carboxylic Acid (19): IR (Ar, 10 K) 3578 (2), 3570 (10), 2165 (2), 2142 (100), 2128 (4), 1758 (21), 1540 (6), 1416 (2), 1350 (3), 1264 (2), 1216 (4), 1149 (10), 1143 (2), 1139 (5), 1103 (4), 1068 (3), 767 (2), 746 (2), 735 (2), 653 (2), 568 (4), 533 (2), 505 (2) cm⁻¹ (relative intensity).

Computational Methods. CCSD(T)[24] geometry optimizations based on analytical energy gradients have been carried out for **1**, **9a**, **2**, and **10a** using the standard 6-31G(d,p) basis set.[23] Vibrational frequencies and infrared intensities of **2a** have been obtained by combining analytical and numerical derivative techniques. Calculations have been repeated at the DFT level with Becke's three-parameter functional B3LYP[21] for which analytical first and second derivatives are available.

Calculated vibrational modes were investigated using the adiabatic mode analysis of Konkoli and Cremer.[27] This approach is based on a decomposition of normal modes in terms of adiabatically relaxed internal parameter modes that are not contaminated by any other mode of the molecule. As has been shown previously, the adiabatic mode analysis is superior to the potential energy distribution (PED) analysis and provides reliable internal frequencies that can directly be assigned to the internal parameters of a molecule.[27] For all molecules considered, zero point energy (ZPE) and thermal corrections have been determined to evaluate reaction enthalpies at 298 K. Calculations were carried out with the COLOGNE96,[40] ACES,[41] and GAUSSIAN94 ab initio packages.[42]

X-ray Crystal Structure Determination of 7c: Siemens P4 diffractometer, graphite monochromator, Mo Kα radiation (λ = 0.710 73 Å), SHELXS-86 program for structure solution by direct methods and SHELXL-93 program for refinement by full-matrix least-squares techniques against F.[243, 44]

Crystal Data: $C_{11}H_{12}N_2O_3$, M = 219.2, monoclinic, space group $P2_1/c$ (no. 14) with a = 9.154(2), b = 10.377(2), c = 11.362(2) Å, β = 93.69(3)°, V = 1077.1(4) Å³, Z = 4, $F(000)$ = 460, D_{calc} = 1.352 g·cm⁻³. Intensity data were collected using ω scans at T = 218 K on a Siemens P4 diffractometer for a yellow crystal of dimensions 0.24 × 0.36 × 0.78 mm with Mo Kα radiation (λ = 0.7173 Å, μ = 0.100 mm⁻¹) in the range 2.66 ≤ 0 ≤ 22.56° (−9 ≤ h ≤ 9, −11 ≤ k ≤ 11,

(40) Kraka, E.; Gauss, J.; Reichel, F.; He, Zhi; Olsson, L.; Konkoli, Z.; Cremer, D. *COLOGNE 96*; Göteborg, Sweden, 1996.

(41) Stanton, J. F.; Gauss, J.; Watts, J. D.; Lauderdale, W. J.; Bartlett, R. J. *ACES II, Quantum Theory Project*; ACES II: University of Florida, FL, 1992.

(42) Frisch, M. J.; Head-Gordon, M.; Trucks, G. W.; Foresman, J. B.; Schlegel, H. B.; Raghavachari, K.; Robb, M. A.; Binkley, J. S.; Gonzalez, C.; Defrees, D. J.; ox, D. J.; Whiteside, R. A.; Seeger, R.; Melius, C. F.; Baker, J.; Martin, R. L.; Kahn, L. R.; Stewart, J. J. P.; Topiol, S.; Pople, J. A. *Gaussian 94*; Gaussian Inc.: Pittsburgh, PA, 1994.

(43) (a) Sheldrick, G. M. *SHELXS 86, A Program for Structure Determination*, Göttingen, 1986. (b) Sheldrick, G. M. *SHELXS 93, A Program for Structure Refinement*, Göttingen, 1993.

(44) Atom coordinates (× 10⁴) with equivalent isotropic displacement parameters (Å² × 10³). U_{eq} is defined as one-third of the trace of the orthogonalized U_{ij} tensor.

$0 \leq l \leq 12$). Three control reflections monitored at regular intervals during data collection displayed no significant deviations in intensity.

Semiempirical absorption corrections were performed using ψ scan data. The structure was solved by direct methods using SHELX-86[43a] and refined against F^2 with SHELX-93[43b] for 1401 independent reflections (from 1498 measured, $R_{int} = 0.051$) to $R = 0.061$ [$I > 2\sigma$-(I)], $wR2 = 0.160$ [all data][44] and $S = 0.907$ [goodness-of-fit]. Hydrogen atoms were included at calculated positions with group isotropic temperature factors. All other atoms were refined anisotropically. The largest difference synthesis peak and hole $\Delta\rho$ were respectively 0.200 and -0.193 Å^{-3}.

Supporting Information Available: Tables of crystallographic data, atomic coordinates, anisotropic and isotropic displacement parameters, the package diagram of quinone diazide **7c**, and the calculated IR spectra of **2** and **10a** (6 pages). See any current masthead page for ordering and Internet access instructions.

JA971731A